27 Apr 1981, 10:30 am - 1:00 pm

Dynamic Triaxial and Vibratory In-Situ Behavior of Cohesive Soil

M. S. El-Hosri
Ecole Centrale des Arts et Manufactures, Paris, France

J. Biarez
Ecole Centrale des Arts et Manufactures, Paris, France

P. Y. Hicher
Ecole Centrale des Arts et Manufactures, Paris, France

Dynamic Triaxial and Vibratory In-Situ Behavior of Cohesive Soil

M. S. El-Hosri, J. Biarez, and P. Y. Hicher
Ecole Centrale des Arts et Manufactures, Paris, France

SYNOPSIS .- In-situ and laboratory shear modulus data are presented and compared. In-situ tests included the cross-hole seismic survey at a stiff marl site, while laboratory tests included the cyclic triaxial test on undisturbed specimens obtained from the same site. The cyclic triaxial device presented in this investigation has been developed and improved so that the reliable response of soil can be measured directly from the specimen over a large range of strain (from 10^{-6} to 10^{-2}).

A series of cyclic triaxial tests were performed under stress controlled condition over a range of frequency from 0,5 to 10 Hz on marl samples consolidated anisotropically. Values of shear modulus and damping ratio are determined for shearing strain amplitude between 10^{-6} and 10^{-2} and compared with published results proposed by Seed and Idriss (1970) and Hardin and Drnevich (1972) At low strains, the shear modulus values measured by in-situ and laboratory methods were in a good agreement, but the values from the Hardin-Black's equation were underestimated. The influence of consolidation stress, frequency, and number of load cycles on the shear modulus have also been investigated.

INTRODUCTION

Ground responses during earthquekes and vibratory loadings are mainly determined by shear modulus and damping ratio of soil deposits.

Various test devices have been developed and improved in recent years to determine shear modulus and damping ratio in both laboratory and in-situ. The most of these devices have certain advantages as well as limitations. The cross-hole seismic survey is well suited for determining the variation of in-situ shear wave velocity (from which G_{max} may be calculated using elastic theory) with depth. For laboratory measurements of dynamic soil behavior, the resonant column device has usually been employed for strain levels of the ordre of 10^{-4} and less. The cyclic triaxial test has seldom been utilized because of the difficulties of making reliable measurements corresponding to a smaller strain level than 10^{-4}. However, reliable dynamic soil behavior corresponding to wide strain level ranging from 10^{-6} to 10^{-2} would be obtained from cyclic triaxial tests if the mechanical frictions related with the measurement of load and displacement could be eliminated.

CROSS-HOLE SURVEY AT THE SITE

The basic principales of the seismic cross-hole survey as described by Stokoe and Woods (1972) were utilized in this investigation. Three vertical borholes were used, one for the impulse and two for receiving. The distance between borholes was about 10 meters to minimize the effects of wave refraction. A vertical velocity transducer was attached to the top of the impulse rod at ground surface and connected to the trigger device of the oscilloscope. Another vertical velocity transducer was fixed to the PVC casing grouted at each receiving hole. The cross-hole measurements were generally recorded at a three meter intervals. At each level investigated and for each receiving hole, different oscilloscope setting of sweep rates and amplitudes were employed to determine the arrival times as accurately as possible. The total travel time determined at each test includes the time for the compression wave to travel down the impulse rod, as well as the travel time of the body waves through the soil from the impulse hole to receiving hole. The impulse rod was calibrated to determine the wave velocity in the rod, and hence, the travelling time in the length of the impulse rod. Consequently, the wave velocities may be calculated using the following relation.

$$V = \frac{L}{t - Kl} \qquad (1)$$

where, V = wave velocity, L = distance between the impulse hole and receiving hole, t = total travel time as recorded from the oscilloscope, l = lengh of the impulse rod, K = calibration factor which is equal to 0.198 m sec/m.

CYCLIC TRIAXIAL TEST

Apparatus. - The basic concept of this test is to create cyclic sollicitations on a specimen placed in a modified triaxial cell which enables us to measure directely the load and displacement (Fig.1).

A load cell rigidly fixed between the top cap of the specimen and the piston, inside the tria-

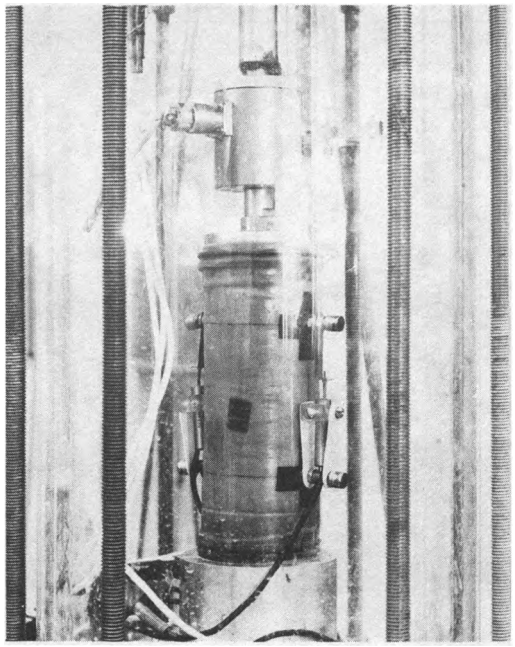

Fig.1 - Cyclic Triaxial Device

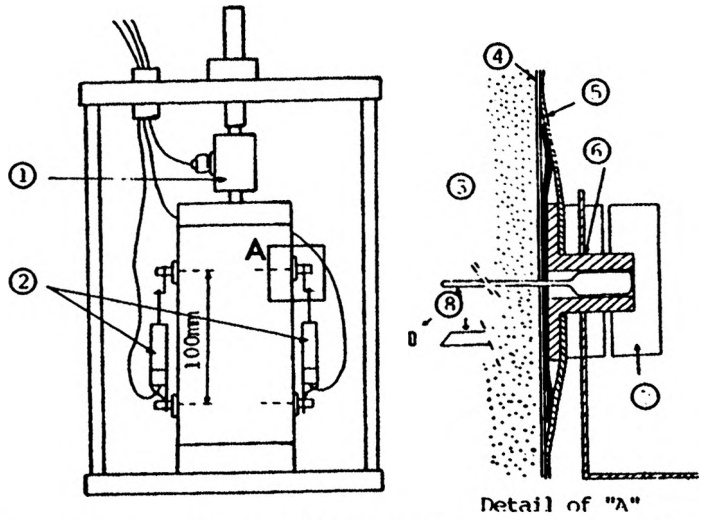

1-Load Cell. 2-Linear Variable Differential Transducers 3-Specimen Soil. 4-First Membrane. 5-Second Membrane. 6-Valve. 7-Tighting Plug. 8-Thin Rod.

Fig.2 - Diagram of improved cyclic triaxial device.

xial cell. This position eliminates any error introduced in the load measurement by the effect of piston-bush friction. The piston of the triaxial cell is connected to the ram of a M.T.S. machine. This load cell is used in the load control test. Two highly sensitive linear variable differential transducers have been attached symmetrically to the specimen by valves fixed at the membrane. The average reading of the two LVDT has been taken as a measurement of displacements to eliminate the effects of uneven movement. Thin rods were introduced in the valves and penetrated inside the specimen to ensure perfect contact between the specimen and the transducer as shown in Fig.2. For small strain levels, exterior measurements do not usually give the reliable response of the material, because of the progressive penetration of the porous stones inside the material, and the bad contacts between the top and base platens and the porous stones.

This method of measurement is indispensable to carry out tests at a very small amplitude strain and stress. By this apparatus we could measure axial strain level ranging from 0.0001 % to 2 %.

A servohydraulic system manufactured by Materials Testing Systems machine was used to apply loads for all tests shown in Fig.3. The hysteresis loops of the axial stress versus the axial strain were drawn on a chart of a x-y recorder.

Soil Specimens. - In-situ undisturbed specimens of stiff marl were teken from borings at depths of 20 to 50 m. The average value of liquid limit was 40 % and plasticity index 28 %. Average consolidated undrained shearing strength parameters (effective stress) were approximately C' = 0 and $\phi' = 38°$.

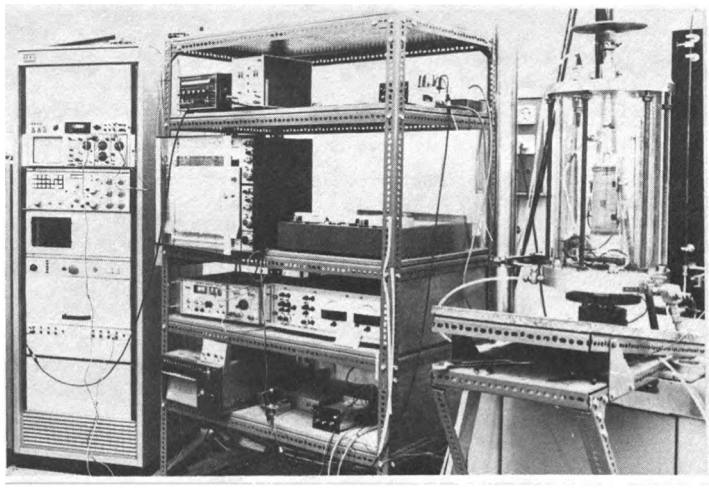

Fig.3 -General View of Experimental Apparatus

Consolidation of Specimens. - Specimens of 70 mm in diameter and 150 mm in height were initially consolidated anisotropically in the triaxial cell during 3-4 days under stresses that were found at in-situ conditions. The value of the coefficient of lateral stress at rest, K_o, was estimated nearly equal to 0.5, and mean effective stress, $\bar{\sigma}_o$, was taken equal to :

$$\bar{\sigma}_o = \frac{\bar{\sigma}_v + 2\bar{\sigma}_h}{3} \qquad (2)$$

where, $\bar{\sigma}_v$: vertical effective stress

$\bar{\sigma}_h$: horizontal effective stress.

Data of the specimens are given in table I.

Table I - Soil Specimens Data

N° specimen	Depth (m)	Dry Unit Weight γ_d gr/Cm³	Void Ratio e	Consolidation Stress		
				$\bar{\sigma}_v$ KPa	$\bar{\sigma}_h$ KPa	$\bar{\sigma}_o$ KPa
1	24.0	1.69	0.56	240	115	157
2	34.0	1.70	0.55	340	160	220
3	41.0	1.70	0.55	410	190	263
4	48.5	1.71	0.54	485	230	315

Testing procedure. - Vertical stress controlled consolidated undrained cyclic test of sinusoid signal were performed on the undisturbed specimens at frequencies of 0.5, 2, 5 and 10 H_z. All specimens were subjected to an increasing series of cyclic deviator stress σ_{dc}. Initial value of $\sigma_{dc} = \pm 1$ KPa, to obtain the smallest possible strains, was used and was then progressively increased to account for large cyclic strains. Each specimen was generally subjected to 20-30 cycles of loading at a given cyclic stress, σ_{dc}, mean effective stress, and frequency of loading. The young's modulus and damping ratio for each loading condition were determined at the 10 th cycle.

TEST RESULTS

RESULTS OF IN-SITU MEASUREMENTS

The shear wave velocities were measured from two receiving borholes at the same depth. From these measurements, the dynamic shear modulus has been calculated using the following equation :

$$G_{max} = \frac{\gamma_t}{g} V_s^2 \qquad (3)$$

where, γ_t = total unit weight of soil, g = acceleration of gravity, and V_s = shear wave velocity.

The variation of the dynamic shear modulus with depth for two locations is shown in Fig.4. It can be seen that the G_{max} increases with depth and the values of G_{max} measured from second boring are higher than those obtained from the firts boring. This indicated that the soil between the three borholes is not homogeneous. The average measurements are presented in Fig.4 by dashed line.

RESULTS OF LABORATORY TESTS

Typical test results for one cycle of leading are expressed by the loop of stress-strain relationship as shown in Fig.5. The slope of the line through the end points of the loop will be called the young's modulus, E, while the half of strain produced from one loop is called

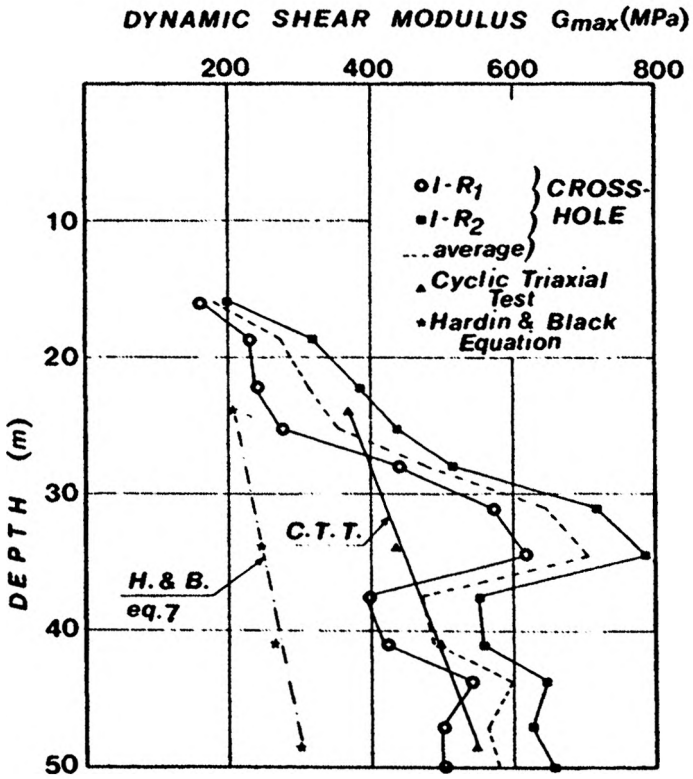

Fig.4 - Low-Amplitude shear modulus as function of depth.

the cyclic axial strain, ε_c. The damping ratio, D, may be determined as follows :

$$D = \frac{A_L}{4 . A_T} \qquad (4)$$

where, A_L = Area of the loop representing the total dissipated energy per cycle, and A_T = triangular area shown cross hatched in Fig.5 representing the work capacity per cycle.

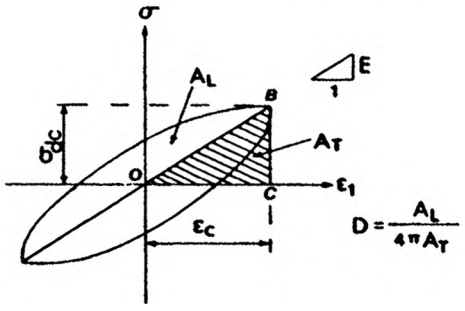

Fig. 5. Definition of young's modulus and damping ratio

In order to compare the laboratory and in-situ results, both young's modulus, E, and cyclic axial strain, ε_c, obtained from cyclic triaxial tests were converted into shear modulus, G, and shearing strain, γ, by using the following equations :

$$G = \frac{E}{2(1+\upsilon)} \qquad (5)$$

$$\gamma = \varepsilon_c (1+\upsilon) \qquad (6)$$

where υ = Poisson's ratio and is teken equal to 0.47 from the average measurement in-situ.

Fig.6 shows the shear strain on a logarithmic graph obtained from 4 tests run under mean effective stresses of consolidation ranging from 157 to 315 KPa at a frequency equal 2 Hz. This figure demonstrated clearly :

- The existance of a maximum constant shear modules value, G_{max}, below a threshold shearing strain of about 5×10^{-6}.

- Above the threshold shearing strain, the shear modulus begins to decrease with increasing the shearing strain amplitude.

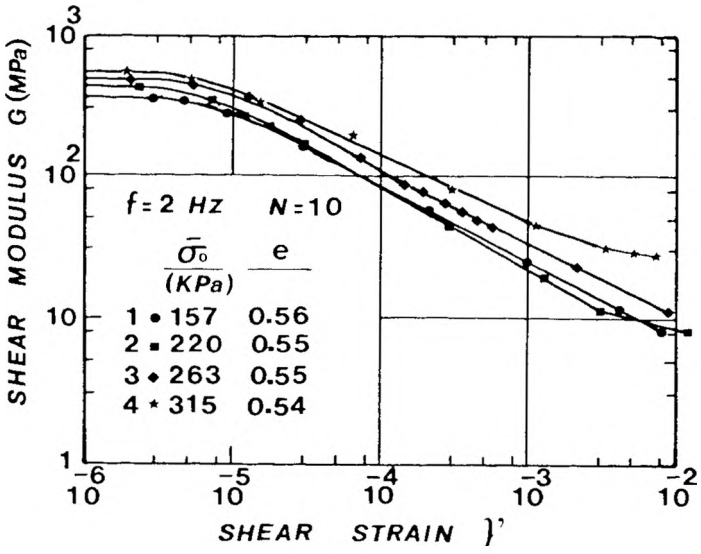

Fig.6 - Shear modulus versus shear strain amplitude for undisturbed specimens of marl.

Fif.7 shows the variation of the damping ratio, D, as a function of shearing strain amplitude for the same tests of which the modulus measurements shown in Fig.6. The solid line represents the average of data. This figure indicates that the damping ratio increases as the strain amplitude increases, which means that the nature of damping is hysteretic. The hysteresis loops of the stress-strain relation show that the damping of this marl involves a plastic part, as the hysteresis loops do not close on itself and present conclusively irreversible strains even that the strain level was about 10^{-6}.

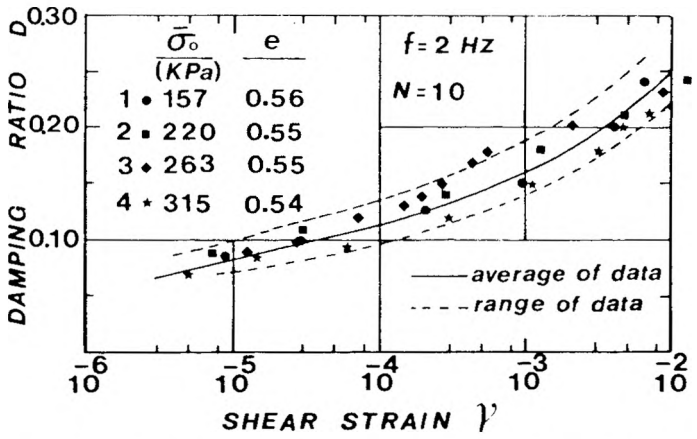

Fig.7 - Damping ratio versus shear strain amplitude for undisturbed specimens of marl.

Influence of Consolidation Stress. - The maximum shear modulus, G_{max}, increases as the mean effective stress of consolidation, $\bar{\sigma}_o$, increases. Fig.8 shows that the relationship between G_{max} at $\gamma = 10^{-6}$ and $\bar{\sigma}_o$, on a logarithmic graph, is linear. The slope of the line is 0.55. Hardin and Drnevich (1972) suggested that for most of soils the slope of the line is 0.50

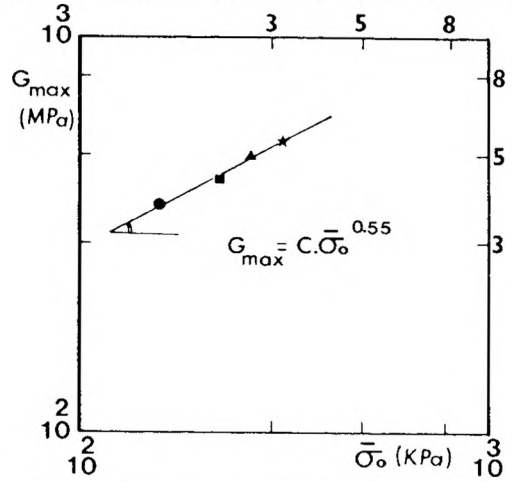

Fig.8 - Influence of consolidation stress on shear modulus at low-amplitude strain

Influence of Frequency. - To determine the influence of frequency on shear modulus, tests have been conducted under the same conditions of consolidation stress and at different frequencies (0.5, 2, 5 and 10 Hz). The results show that the shear modulus increases slightly with increasing frequency over the considered range.

Influence of Number of Load Cycles. - The influence of number of load cycles on shear modulus for this marl depends on the shearing strain level. At shearing strain less than 10^{-4}, the shear modulus slightly decreases between the first and fifteenth cycle, and beyond that the shear modulus becomes constant.

COMPARISON OF VALUES OF SHEAR MODULUS AT LOW STRAINS

In Fig.4, the values of the shear modulus, G_{max} measured by the in-situ seismic method are compared directly with values of G_{max} corresponding to $\gamma = 10^{-6}$ obtained from cyclic triaxial tests, and the values of G_{max} estimated by the empirical equation derived by Hardin and Black (1968 and 1969) :

$$G_{max} = 3{,}23 \frac{(2.97-e)^2}{1+e} \bar{\sigma}_o^{0.5} (OCR)^K \quad (7)$$

where, G_{max}, is in MPa, $\bar{\sigma}_o$ = mean effective confining stress in KPa, e = void ratio, OCR = overconsolidation ratio, K = parameter depends on soil plasticity index.

The figure clearly indicates a good agreement between in-situ measurements and cyclic triaxial laboratory results. It can also be seen that the values of Gmax estimated from equation (7) are about 50 % of both in-situ and laboratory values. It would appear, therefore, that this equation anderestimated the shear modulus of this stiff marl.

COMPARISON OF LABORATORY DATA WITH SOME PUBLISHED DATA

The shear modulus, G, normalized by the modulus G_{max}, at $\gamma = 10^{-6}$ extrapolated from the curves in Fig.6 are shown as a function of the logarithm of shearing strain amplitude in Fig.9. A single solid line represents the average of data as the effect of consolidation stress is not significant on the examined specimens due to its narrow range.

The average curve of the damping ratio versus shear strain presented in Fig.7 is plotted in Fig.10 along with some published data for comparison.

The typical curves suggested by Seed and Idriss (1970) for clays and peats showing the variation of the normalized shear modulus and damping ratio with strain amplitude are presented in Fig.9 and 10 respectively, where G_{max} is the shear modulus at $\gamma = 3 \times 10^{-6}$.

The curves of normalized shear modulus and normalized damping ratio versus shear strain suggested by Hardin and Drnevich (1972) were based on the hyperbolic stress-strain relationship. The normalized shear modulus is given by :

$$\frac{G}{Gmax} = \frac{1}{1+\gamma_h} \quad (8)$$

and the normalized damping ratio :

$$\frac{D}{D_{max}} = \frac{\gamma_h}{1+\gamma_h} \quad (9)$$

where D_{max}, is the maximum value of the damping ratio, and γ_h is the hyperbolic shearing strain determined by.

$$\gamma_h = \frac{\gamma}{\gamma_r} \left(1 + a e^{-b (\gamma/\gamma r)} \right) \quad (10)$$

in which a and b are soil constants, e is the base of natural logarithm, and γ_r is the reference strain difined by.

$$\gamma_r = \frac{Tmax}{Gmax}$$

where Tmax is the maximum shearing strength, Gmax value is determined by equation (7), and D_{max}, a and b values for cohesive soils are given by Hardin and Drnevich.

Using equations 8 and 9, the curves of variation of G/G_{max} and damping ratio with shear strain for the specimen N° 1 and 4 were established and are shown by dashed lines in Figs.9 and 10.

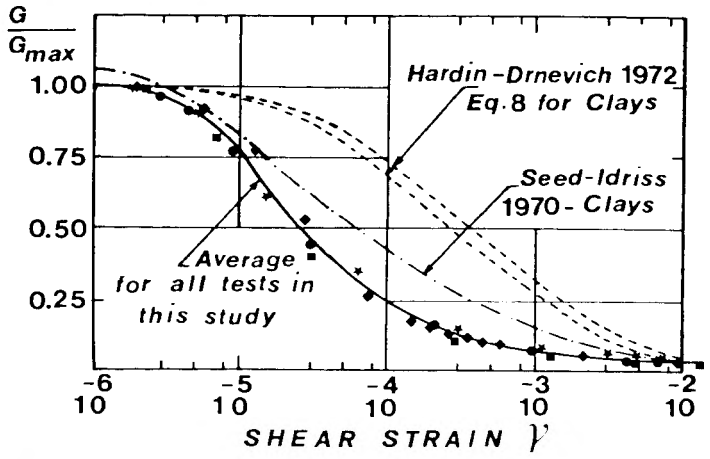

Fig.9 - Normalized shear modulus versus shear strain for undisturbed specimen of marl compared with some published data

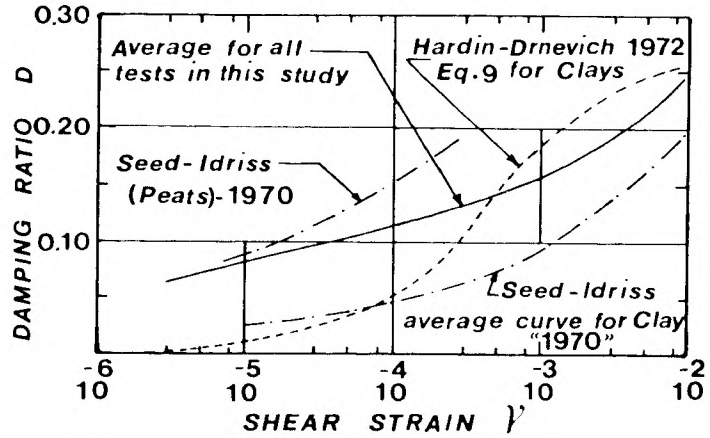

Fig.10 - Damping ratio versus shear strain for undisturbed specimens of marl compared with some published data.

It can be seen from Fig.9 that the reduction of the shear modulus with strain amplitude for this marl is much higher than that predicted for cohesive soils from equation (8) and slightly higher than the typical curve proposed by Seed-Idriss for clays. It can also be seen in Fig.10 that the curve of damping ratio versus shear strain for this marl is higher than the average curve for clays, and less than the curve for peats, both proposed by Seed and Idriss. Whereas, it is much higher than the curve for cohesive soils obtained from equation (9) at strain levels less than $3x10^{-4}$. It should be noted that Hardin and Drnevich suppose in the previous equations that soils have a nearly perfectly elastic behavior for a shear strain about 10^{-5}.

For a material purely elastic, the loop of stress-strain relationship is presented by a line, which means that the energy is stored during leading and released entirely during unloading without any energy dissipated, and consequently the G/Gmax equal to unity for any level of strain amplitude. But since the loop stress-strain presents some dissipated energy, the material is no more perfectly elastic and G/G_{max} decreases. This reduction of G/G_{max} increases as long as the dissipated energy increases.

We have above seen that the nature of damping for this marl is hysteretic, it increases with increasing shear strain, and involves a plastic part. We have also shown in Fig.10 that the values of damping ratio at strain levels less than 10^{-4} for this marl are higher than those proposed by Seed and Idriss and by equation (9) for clays. These reasons, may explaine the strong reduction of G/G_{max} for marl by comparaison with other curves shown in Fig.9.

CONCLUSION

1. The shear modulus values at low-amplitude strains for the stiff marl, determined from improved cyclic triaxial test, are in good agreement with those measured in-situ using the seismic cross-hole method.

2. Shear modulus values, calculated using equation (7) proposed by Hardin and Black, are nearly 50 percent of those measured both in-situ and laboratory for a low-amplitude strain.

3. Above a threshold shearing strain level of about $5x10^{-4}$, shear modulus decreases while damping ratio increases with increasing shearing strain amplitude.

4. The nature of damping for this marl is hysteretic and it involves a plastic part.

5. The relationship between the maximum shear modulus, Gmax, and the mean effective stress $\bar{\sigma}_0$, appears to be linear on a logarithmic plot ; the slope of which is 0.55.

6. The shear modulus slightly increases with frequencies between 0,5 and 10 Hz.

7. The shear modulus does not appear to be influenced by the number of load cycles for strain levels smaller than 10^{-4}, but it slightly decreases between the first and fifteenth cycle for higher strain levels.

8. The rate of decrease of the shear modulus with shear strain for the investigated marl was found higher than that proposed by Hardin and Drnevich (1972) and Seed and Idriss (1970) for clays.

9. The values of damping ratio obtained in the present investigation were found in between those values estabilised by Seed and Idriss for peats and clays.

REFERENCES

BIAREZ,J., GRIMM, D., and EL-HOSRI, M.S. (1978) "Dynamic Behavior of Cohesive Soil", Internal Report, Ecole Centrale de Paris (in French).

EL-HOSRI, M.S. (1979), "Contribution to the Study of the Mechanical Properties of Materials under Cyclic Loading," Dr. Engineer Thesis, Ecole Centrale de Paris (in French).

HARDIN,B.O., and BLACK,W.L. (1968), "Vibration Modulus of Normally Consolidated Clay", J. SMFD, Proceedings ASCE, Vol. 94, SM2, March, pp. 353-369.

HARDIN,B.O., and BLACK, W.L. (1969), "Closure to "Vibration Modulus of Normally Consolidated Clay", J. SMFD, Proceedings ASCE, Vol.95, N° SM6, Novembre, pp. 1531-1539.

HARDIN,B.O. and DRNEVICH.V.P. (1972), "Shear Modulus and Damping in Soil : Measurement and Parameter Effects", J.SMFD, Proceedings ASCE, Vol.98, N° SM6, June, pp.603-624.

HARDIN,B.O., and DRNEVICH,V.P. (1972, "Shear Modulus and Damping in soil ; Design Equations and Curves", J. SMFD, Proceedings ASCE, Vol.98, N° SM7, July, pp. 667-692.

RICHART,F.E., HALL, J.R., and WOODS,R.D.(1970) "Vibrations of Soils and Foundations," Prentice-Hall, Inc., Englemood Cliffs, N.J.

SEED,H.B., and IDRISS, I.M. (1970), "Soil Moduli and Damping Factors for Dynamic Response Analyses", Earthquake Engineering Research Center, University of California, Berkeley, California, Report N°. EERC 70-10.

STOKOE,K.H., and WOODS,R.D. (1972), "In situ Shear Wave Velocity by Cross-Hole Method", J. SMFD, Proceedings ASCE, Vol. 98, N° SM5, May, pp. 443-460.